

Förster resonance energy transfer mediated enhancement of the fluorescence lifetime of organic fluorophores to the millisecond range by coupling to Mn-doped CdS/ZnS quantum dots

This content has been downloaded from IOPscience. Please scroll down to see the full text.

2016 Nanotechnology 27 055101

(<http://iopscience.iop.org/0957-4484/27/5/055101>)

View [the table of contents for this issue](#), or go to the [journal homepage](#) for more

Download details:

IP Address: 46.5.0.243

This content was downloaded on 22/03/2016 at 16:32

Please note that [terms and conditions apply](#).

# Förster resonance energy transfer mediated enhancement of the fluorescence lifetime of organic fluorophores to the millisecond range by coupling to Mn-doped CdS/ZnS quantum dots

Uwe Kaiser<sup>1</sup>, Nadeem Sabir<sup>1</sup>, Carolina Carrillo-Carrion<sup>1</sup>, Pablo del Pino<sup>2</sup>, Mariano Bossi<sup>3</sup>, Wolfram Heimbrot<sup>1</sup> and Wolfgang J Parak<sup>1,2</sup>

<sup>1</sup> Department of Physics and Material Sciences Center (WZMW), Philipps-University Marburg, Renthof 5, D-35032 Marburg, Germany

<sup>2</sup> CIC biomaGUNE, Paseo de Miramón 182, 20009, Donostia—San Sebastián, Spain

<sup>3</sup> CONICET, Pabellón 2, Piso3, Ciudad Universitaria, Buenos Aires, Argentina

E-mail: [Wolfram.Heimbrot@physik.uni-marburg.de](mailto:Wolfram.Heimbrot@physik.uni-marburg.de) and [Wolfgang.Parak@physik.uni-marburg.de](mailto:Wolfgang.Parak@physik.uni-marburg.de)

Received 7 September 2015

Accepted for publication 10 November 2015


Published 16 December 2015



CrossMark

## Abstract

Manganese-doped CdS/ZnS quantum dots have been used as energy donors in a Förster-like resonance energy transfer (FRET) process to enhance the effective lifetime of organic fluorophores. It was possible to tune the effective lifetime of the fluorophores by about six orders of magnitude from the nanosecond (ns) up to the millisecond (ms) region. Undoped and Mn-doped CdS/ZnS quantum dots functionalized with different dye molecules were selected as a model system for investigating the multiple energy transfer process and the specific interaction between Mn ions and the attached dye molecules. While the lifetime of the free dye molecules was about 5 ns, their linking to undoped CdS/ZnS quantum dots led to a long effective lifetime of about 150 ns, following a non-exponential transient. Manganese-doped core-shell quantum dots further enhanced the long-lasting decay time of the dye to several ms. This opens up a pathway to analyse different fluorophores in the time domain with equal spectral emissions. Such lifetime multiplexing would be an interesting alternative to the commonly used spectral multiplexing in fluorescence detection schemes.

 Online supplementary data available from [stacks.iop.org/NANO/27/055101/mmedia](http://stacks.iop.org/NANO/27/055101/mmedia)

Keywords: energy transfer, time-resolved fluorescence, quantum dots

(Some figures may appear in colour only in the online journal)

## 1. Introduction

Using quantitative fluorescence [1, 2] for the detection of fluorophores is a common method for quantifying the concentration of analytes in a solution, e.g. via fluorescence-labelled antibodies which selectively bind to the analyte [3], or by using analyte-sensitive fluorophores [4, 5]. By using several fluorophores in parallel, in principle the concentration

of different analytes can be determined simultaneously. This is possible by using fluorophores with a different colour of emission, although this is hampered by spectral overlap as determined by the bandwidth of the emission of the different fluorophores [1]. Alternatively, discriminating the fluorescence emission of different fluorophores can also be achieved in the time domain [6]. In cases where fluorophores possess different emission lifetimes, their emission can be

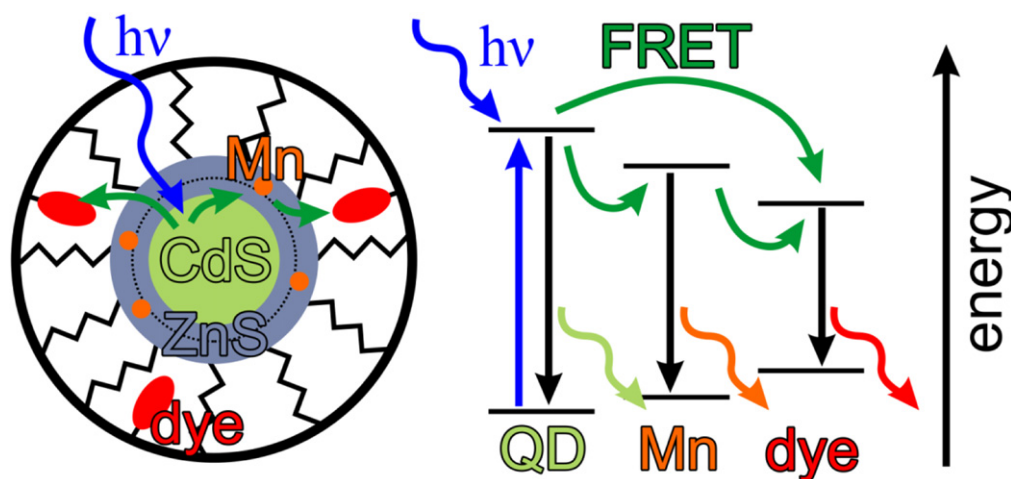


**Figure 1.** On the left, a sketch of the Mn-doped CdS/ZnS QDs with attached dye molecules is shown. The Mn ions are incorporated within the ZnS shell. A scheme of the different energetic states is depicted on the right. The excitation of the CdS core is indicated by the blue wavy arrow. The green arrows show the possible energy transfer pathways. The QD, the Mn ions, and the dye can all undergo radiative recombination to the respective ground state under the emission of photons.

distinguished via time-dependent fluorescence measurements. This principle is used for fluorescence lifetime imaging, for example, in which the lateral distribution of different fluorophores is detected by the deconvolution of the respective recorded emissions in the time domain [7]. Unfortunately, variation in the fluorescence lifetime of organic fluorophores is limited, typically within a range of a few nanoseconds. This lies within the same region as the autofluorescence lifetimes of biological samples such as cells [8]. The use of inorganic fluorophores based on quantum dots (QDs) allows for slightly higher fluorescence lifetimes. QDs can be combined with other fluorophores in Förster-like resonance energy transfer (FRET) schemes. In cases where lanthanides are used as donors and QDs as acceptors, a multiplexed read-out of fluorescence with long lifetimes is possible [9, 10]. Alternatively, QDs can be used as donors for organic fluorophores as acceptors [11, 12]. Based on the last detection scheme, we have recently shown that lifetime multiplexing is an interesting alternative to spectral multiplexing. In this previous work, ATTO590 dye molecules bound to gold nanoparticles (NPs) exhibited a mono-exponential decay with a lifetime of a few ns (equivalent to the lifetime of free dye molecules), whereas dye molecules bound to CdSe/ZnS QDs showed a non-exponential decay with a slow component of more than 100 ns due to the FRET from the QDs to the dye. We demonstrated the fundamental possibility of determining the mixing ratio for dyes with equal luminescence spectra but very different transients [13]. The doping of CdS/ZnS QDs with Mn ions leads to long-lived fluorescence lifetimes based on the dipole forbidden internal 3d-transition [14, 15]. In the present paper we demonstrate that in this way the fluorescence decay time of organic fluorophores can be shifted up to the ms time scale by coupling them to Mn-doped CdS/ZnS QDs.

## 2. Methods

In order to demonstrate the double energy transfer process among the three luminescence centres—first within the Mn-doped CdS/ZnS QDs, i.e. from the CdS/ZnS matrix to the Mn ions, and then second from the excited Mn ions to an organic dye—we conjugated the organic fluorophore ATTO633 to the surface of the Mn-doped CdS/ZnS QDs, see figure 1. For this purpose, firstly undoped and Mn-doped CdS/ZnS core-shell QDs were synthesized in the organic phase, as adopted from a previously reported method [16–19]. It must be pointed out that the Mn ions were incorporated into the ZnS shell and not the CdS core, followed by an additional ZnS shell which was grown on top of the doped shell. We thus refer to these NPs as CdS/Mn:ZnS/ZnS QDs. Transfer of the hydrophobic QDs to the aqueous phase was then achieved by overcoating the hydrophobic QDs in the organic phase with an amphiphilic polymer, followed by the evaporation of the organic phase and redispersion of the QDs in water, as reported in previous work [20–22]. The used amphiphilic polymer consisted of a polyisobutylene-alt-maleic anhydride hydrophilic backbone modified with dodecylamine hydrophobic side chains (PMA). This polymer wraps around the QDs with its hydrophobic side chains intercalating the hydrophobic surfactant molecules present on the QD surface after synthesis in organic solvent, while its hydrophilic backbone points towards the solution, thus providing colloidal stability. NH<sub>2</sub>-modified ATTO590 (absorption maximum at 594 nm, emission maximum at 624 nm), NH<sub>2</sub>-modified ATTO633 (absorption maximum at 629 nm, emission maximum at 657 nm), or NH<sub>2</sub>-modified ATTO655 (absorption maximum at 663 nm, emission maximum at 684 nm), was directly incorporated into the polymer, and after the polymer coating of the QDs is thus present on the QD surface. In the present work, 2% of the maleic anhydride rings

in the polymer backbone were conjugated with ATTO dye, similar to previous reports [2, 20–23]. After the polymer coating procedure, several purification steps combining filtration and gel electrophoresis were carried out to remove the empty polymer micelles, which form in addition to the polymer-coated QDs as a by-product. For details, refer to the supporting information. Despite purification, some residual polymer micelles containing ATTO dye but with no QDs inside may remain.

Once the QDs had been purified and concentrated (via ultrafiltration) the following QD samples were prepared at the same QD concentration: undoped QDs (CdS/ZnS/ZnS); Mn-doped QDs (CdS/ZnS:Mn/ZnS); undoped QDs with ATTO633 on their surface (ATTO633-CdS/ZnS/ZnS), and Mn-doped QDs with ATTO633 on their surface (ATTO633-CdS/ZnS:Mn/ZnS). All QD samples were characterized by ultraviolet-visible (UV/Vis) absorption spectroscopy and fluorescence spectroscopy (see the supporting information for details). All measurements were performed in water. For spectrally resolved fluorescence measurements, the continuous wave photoluminescence (PL) spectra for the different samples were recorded with a Fluorolog-3 fluorescence spectrometer (model FL3-22, Horiba) under wavelength excitation at 350 nm. These steady-state fluorescence measurements were carried out by working with a sample volume of 30  $\mu\text{l}$  in UV-compatible ultra-micro-cuvettes with a path-length of 1 cm. Time-resolved fluorescence measurements were made with a frequency triple-pulsed Nd:YAG laser operating at a wavelength of 355 nm with a fixed repetition rate of 10 Hz. The decay time of the exciting laser pulse was around 3 ns, which is the lower limit for lifetime determination. A sample volume of 100  $\mu\text{l}$  was used in UV-compatible micro-cuvettes with a path-length of 1 cm. The excited area had a diameter of 1 mm resulting in an excitation density of around  $1 \text{ J m}^{-2}$  per pulse. The PL was collected perpendicular to the excitation and analysed with a 250 mm spectrograph using a 300-line-per-millimetre grating with a blaze wavelength of 500 nm. The resulting spectra were recorded with a gated iStar intensified charge-coupled device (ICCD), featuring a minimum gate width of 2 ns. For measuring long decay times, the gate width of the ICCD was gradually increased when the recorded intensity decreased to the background noise level. Due to this rise in exposure time for long periods after excitation it was possible to achieve a sensitivity of up to nine orders of magnitude. The decay curves were obtained by integrating the intensity of the particular PL band for the spectra measured at different times after the excitation pulse.

### 3. Results

In the first analysis, steady-state emission of the different QD samples was recorded. In figure 2, the normalized PL spectra are depicted for three different conjugates under continuous wavelength excitation at 350 nm. The solid red line shows the PL of undoped CdS/ZnS QDs with attached ATTO633 molecules (QD-ATTO633). The two featured bands can be

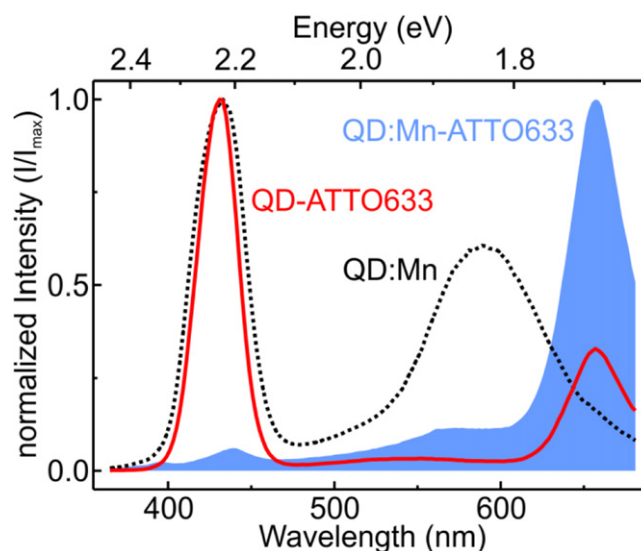


**Figure 2.** Normalized PL spectra are shown for three different QD conjugates under continuous wavelength excitation at 350 nm. The blue area shows the PL of the doped QDs with attached dye molecules (ATTO633-CdS/ZnS:Mn/ZnS), which is dominated by the dye band around 655 nm. The PL of undoped QDs with attached dye (ATTO633-CdS/ZnS/ZnS) is depicted by the solid red line and the PL of doped QDs without dye (CdS/ZnS:Mn/ZnS) is displayed by the dotted black line. All fluorescence spectra show a PL band around 430 nm caused by the QDs.

assigned to QD emission around 430 nm and the dye emission around 655 nm. From the corresponding QD absorption peak at around 392 nm (shown in the SI) the size of the CdS core of the QD was estimated to be 3.1 nm [24], neglecting the shift of the first exciton peak in the absorption spectrum, as well as the increase of the extinction coefficient of the QD upon the growth of a ZnS shell around the core. Corresponding transmission electron microscopy (TEM) results display a mean diameter of  $4.5 \pm 0.8$  nm of the inorganic part of the CdS/ZnS/ZnS QDs (without the organic shell, which does not provide contrast), which is in reasonable agreement with the value determined from the UV/Vis absorption spectra (shown in the SI).

It is known from the literature that when Mn ions are incorporated into the ZnS shell, the quantum yield of Mn emission increases substantially in comparison with Mn dopants inside a CdS core or at the core-shell interface [25]. Moreover, the growth of several additional ZnS layers over CdS/Mn:ZnS (leading to CdS/Mn:ZnS/ZnS) was demonstrated to increase chemical stability, photostability and optical quality in terms of quantum yield [25, 26]. Note that in the present study, no structural analysis regarding the location of the Mn ions in the ZnS shell was performed, as a strict verification of doping would require [27–31]. However, due to synthesis protocol we can assume that the Mn ions are situated within the ZnS shell and not on the QD surface. The dashed black line in figure 2 shows the PL spectrum of the resulting CdS/Mn:ZnS/ZnS QDs. Here, the QD fluorescence at 430 nm is broader in comparison with the PL band of the undoped QDs. This fact indicates a slightly increased size distribution for the doped QDs, as the width of the PL band is

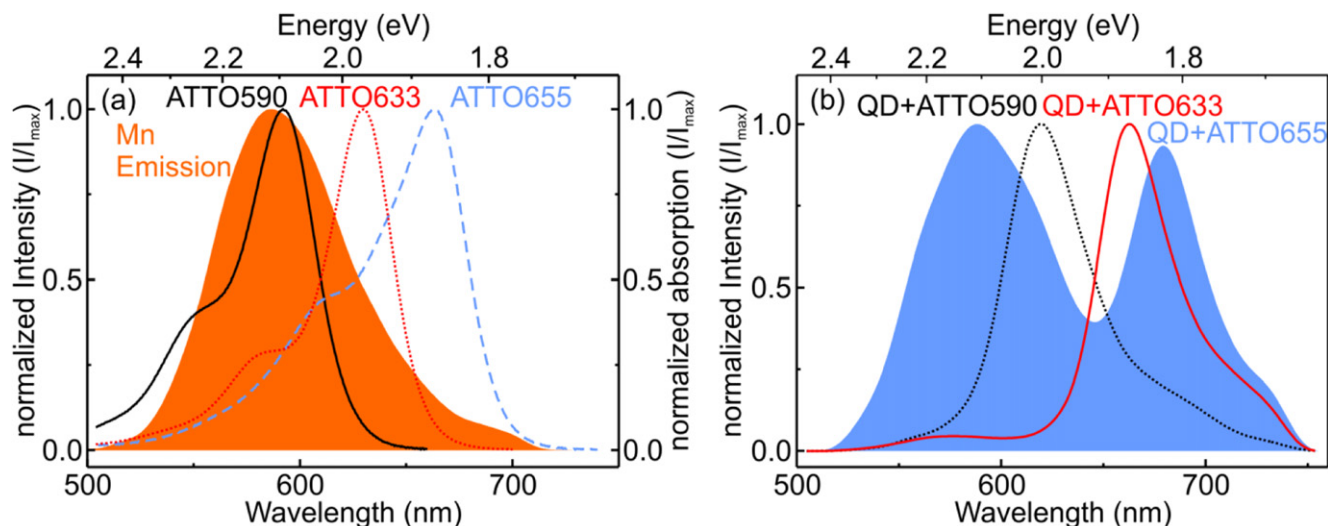


**Figure 3.** (a) The full (orange) area shows the normalized Mn emission ( $I/I_{max}$ ) band of doped CdS/Mn:ZnS/ZnS QDs excited with 355 nm. The lines depict the normalized absorption bands for three different dye molecules, namely ATTO590, ATTO633 and ATTO655. (b) The normalized PL spectra for the Mn-doped QD dye conjugates with the three different dye molecules excited with 355 nm, i.e. ATTO590-CdS/Mn:ZnS/ZnS (black), ATTO633-CdS/Mn:ZnS/ZnS (red), and ATTO655-CdS/Mn:ZnS/ZnS (blue).

mainly determined by their size distribution [32]. The PL band around 590 nm can be assigned to the typical  ${}^4T_1 \rightarrow {}^6A_1$  transition of the Mn ions on cation sites in ZnS [33]. The diameter of the inorganic part of the doped QDs as determined by TEM was  $4.4 \pm 0.7$  nm (shown in the SI), and thus very similar to that of the undoped QDs.

The blue area in figure 2 shows the normalized PL spectrum of Mn-doped CdS/ZnS QDs with attached ATTO633 molecules. The spectrum is dominated by dye emission around 655 nm. Additionally, a Mn emission band around 590 nm can be observed, which only appears as a small shoulder in the low energetic region of the dye PL due to the relatively low intensity. At 430 nm, the PL band originating from the QD core is also visible. The low intensity of the QD fluorescence in comparison to the Mn PL and the ATTO633 bands indicates an effective energy transfer from the QD to the Mn states. The role of the Mn ions within the transfer process cannot be ascertained by continuous wave experiments. For a thorough investigation of the interaction between the Mn ions and the attached dye molecules, a study on Mn-doped QDs with different dye molecules was performed.

As the spectral overlap between the donor emission and the acceptor absorption is crucial for efficient energy transfer [34], a variation of this overlap was performed by using three different dye molecules with distinct absorption and emission spectra. In figure 3(a) the absorption spectra for the three different dye molecules, i.e. ATTO590, ATTO633 and ATTO655, are shown, which were attached to the CdS/Mn:ZnS/ZnS QDs. It is obvious that the characteristic absorption bands are very similar and differ only in the wavelength of the absorption maximum. Additionally, the normalized Mn emission of the doped QDs is depicted by the orange area. For the ATTO590 dye there is a very high spectral overlap between the Mn emission and the dye absorption, as the respective maxima lie at the same wavelength. Due to the

shifted absorption maximum of the ATTO633 dye, the spectral overlap is clearly reduced, which should lead to a less efficient energy transfer. For the ATTO655 dye this is even more valid.

In figure 3(b) the normalized emission spectra for the three Mn-doped QD dye conjugates with the different dye molecules at a 355 nm wavelength excitation are depicted (i.e. ATTO590-CdS/Mn:ZnS/ZnS, ATTO633-CdS/Mn:ZnS/ZnS, and ATTO655-CdS/Mn:ZnS/ZnS). The spectra were recorded from 10 to 20  $\mu$ s after the pulsed excitation. The dotted black line shows the emission of the doped ATTO590-CdS/Mn:ZnS/ZnS conjugate. Only the typical emission band originating from the dye molecules at around 620 nm is visible. As there is no emission band originating from the Mn ions, this implies a rather effective energy transfer from the Mn to the dye molecules. The spectrum of the ATTO633-CdS/Mn:ZnS/ZnS conjugate is depicted by the solid red line and is dominated by the dye emission as well. Nevertheless, a small band around 590 nm is visible, which can be assigned to the Mn transition. The emission spectrum of the ATTO655-CdS/Mn:ZnS/ZnS conjugate is given by the blue area in figure 3(b). Here, two PL bands of similar intensity are visible, which can be assigned to the Mn and dye emission, respectively. A comparison of these three spectra clearly shows a variation in the effectiveness of energy transfer for the different conjugates. For the highest spectral overlap, energy transfer leads to the disappearance of the Mn band in the ATTO590-CdS/Mn:ZnS/ZnS conjugate. In cases where there is a small overlap integral, the transfer is less effective leading to clearly visible Mn emission.

The rate of QD exciton to Mn state energy transfer was found by others to be strongly dependent on the doping location, i.e. the distance between the CdS core and the Mn ion in the ZnS shell [17]. We refer again to the schematic drawing of the Mn-doped QDs in figure 1. The CdS core is responsible for the typical QD emission band. The CdS core

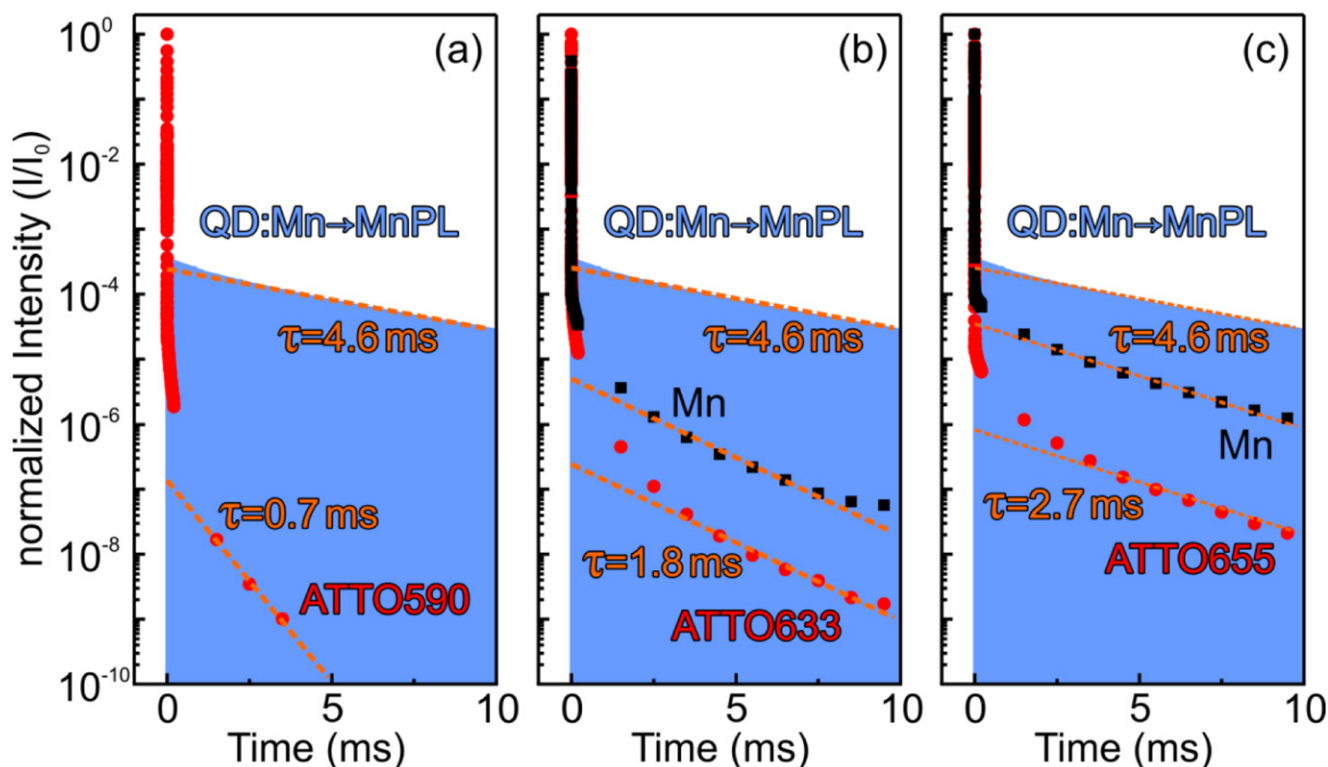


**Figure 4.** The normalized PL decay curves of Mn-doped QD conjugates with attached (a) ATTO590, (b) ATTO633, and (c) ATTO655 molecules are depicted. The full (blue) area in the graphs gives the decay of the Mn PL band at 585 nm for doped QDs without any attached dye molecules excited at 355 nm. The black squares show the Mn PL transient at 585 nm if the dyes are bound to the QD. The red points give the decay of the dyes at (a) 620 nm, (b) 655 nm and (c) 680 nm and the dotted lines represent a mono-exponential fit with the respective lifetimes given in the graph. For the ATTO590-CdS/Mn:ZnS/ZnS conjugate shown in (a), no Mn band was observable, and therefore only the dye PL decay is shown.

is overcoated by a ZnS shell, which is grown in a multi-step process as indicated by the dotted line. During this growth mechanism the Mn ions are incorporated within the ZnS shell [19]. After the additional ZnS shell, this CdS/Mn:ZnS/ZnS core-shell QD is then wrapped with an amphiphilic polymer onto which the dye molecules are attached. The excitation of the QD via impinging light is shown by the wavy line in figure 1, whereas the subsequent energy transfer is depicted by the green arrows. On the right-hand side of figure 1, the respective energy levels and the energy transfer are depicted schematically. It is clear that the excitation of the QD can undergo a direct energy transfer to the dye molecule or a stepwise transfer via the Mn ion. All three energy states corresponding to the three fluorescence emitters, namely that of the QD, the Mn ion and the dye molecule, can undergo a transition into the respective ground state by emitting a photon. The detection of the emitted PL, especially by time-resolved measurements, provides detailed information about the possible transfer processes.

In figure 4 the normalized PL decay curves are given for the different bands for the three conjugates—except for the ATTO590-CdS/Mn:ZnS/ZnS conjugate in (a), where the Mn PL band could not be observed. In all three graphs the decay of the Mn PL at 585 nm for the doped QDs without any attached dye molecules is given by the blue area. The Mn PL shows a fast decay for short times after excitation due to the

transfer of the excitation energy to the defect or trap states [35, 36]. After approximately one millisecond this transfer seems to be irrelevant to further decay characteristics, leading to a mono-exponential decay with a lifetime of about 4.6 ms, as indicated by the dotted line in figure 4. This value is significantly larger in comparison with the radiative lifetime of Mn states reported by others for pure bulk ZnS with very low Mn concentrations, which have been determined to be in the range between 1.8 ms and 2 ms [14, 37]. Higher Mn concentrations usually yield a faster non-exponential decay. From detailed concentration dependence analysis, an intrinsic lifetime of 3.3 ms has been revealed [38]. Longer lifetimes have also been reported for Mn PL in similar QD systems [12, 17, 39]. This can be explained by the influence of the reduced effective refractive index on the transition matrix element for QD materials with extensions much smaller than the emission wavelength [12].

For the conjugates with different dye molecules attached to the Mn-doped QDs we obtained smaller values for the decay times. This reduced lifetime of the Mn PL is proof of the non-radiative energy transfer from the Mn ions incorporated into the ZnS shell of the QDs, as simple reabsorption would not change the lifetime of the Mn donor states. It is obvious that the attached dye molecules operate as an energy acceptor for Mn excitation here. These dye molecules normally show a fast decay with a lifetime of several ns [40].

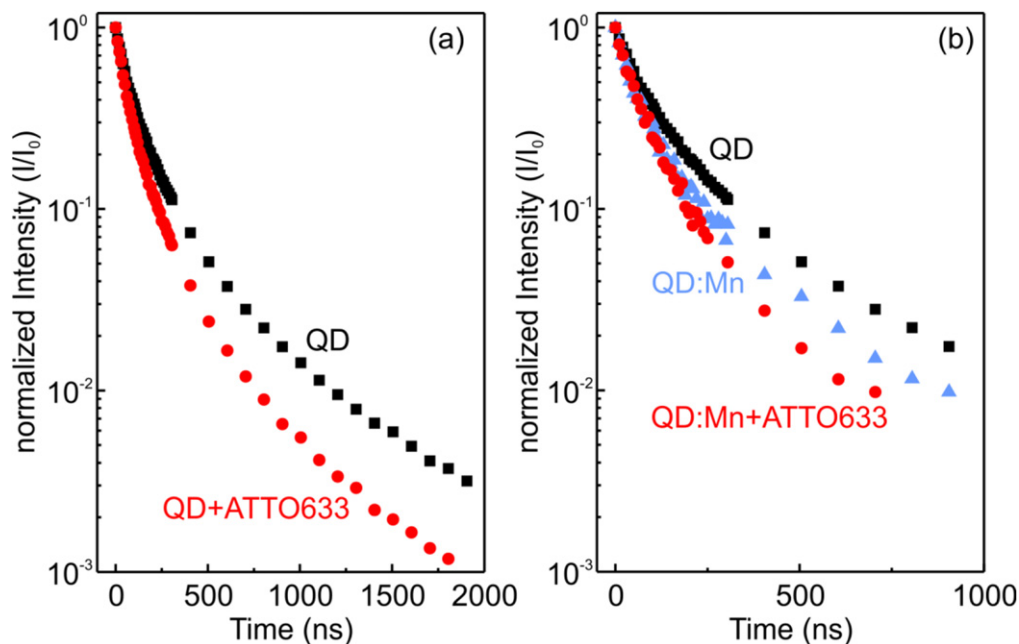


**Figure 5.** Decay curves of the QD PL around 430 nm for different QD conjugates excited at 355 nm. (a) Time behaviour of the QD PL band of CdS/ZnS/ZnS QDs with (red circles) and without (black squares) attached ATTO633 dye molecules. (b) Decay of the QD PL band for CdS/ZnS/ZnS (black squares) and CdS/Mn:ZnS/ZnS (blue triangles) QDs. The QD PL decay for ATTO633-CdS/Mn:ZnS/ZnS QDs (red circles) is also depicted.

Even the coupling to different QDs rarely extends their lifetime to the  $\mu\text{s}$  range [6, 13]. By attaching these molecules to Mn-doped QDs we obtained a dye PL lifetime of several ms. From the determined lifetimes the efficiency of the energy transfer ( $E$ ) can be estimated by the following equation [41]:

$$E = 1 - \frac{\tau_{\text{DA}}}{\tau_{\text{D}}} \quad (1)$$

Here  $\tau_{\text{D}}$  is the lifetime of the donor in the absence of an acceptor and  $\tau_{\text{DA}}$  is the lifetime of the donor in the presence of an acceptor. For the ATTO590-CdS/ZnS:Mn/ZnS conjugate in figure 4(a) we can assume a Mn state lifetime of 0.7 ms, although the PL band is not visible due to the high dye intensity. With equation (1) we get a FRET efficiency of 0.85, 0.61 and 0.41 for the QD conjugates with ATTO590, ATTO633 and ATTO655 dyes respectively. As can be seen in figure 3 efficient energy transfer from the Mn to the dye states leads to a well-observable dye PL band. However, highly effective energy transfer is not always desirable as the energy transfer leads to a reduced lifetime of the Mn PL. This fact eventually limits the accessible lifetimes for the dyes after energy transfer.

For a detailed analysis of the possible transfer pathways, we selected the ATTO633-CdS/ZnS:Mn/ZnS conjugates. As can be seen in figure 1, three energy transitions of the conjugates are relevant, namely the QD excitons, the Mn internal transition and the dye transition. In the following, the time behaviour of the three respective luminescence bands is discussed individually. In figure 5 the transients are depicted. In figure 5(a) the QD PL is compared for CdS/ZnS/ZnS QDs with and without attached ATTO633 dye molecules. The decay is non-exponential in both systems with a PL

observable up to several ms. A significant change in the decay curve can be observed by attaching ATTO633 dye molecules to the CdS/ZnS/ZnS QDs. The QD PL decays faster due to radiationless energy transfer from the QD states to the dye states.

In figure 5(b), the PL decay of CdS/ZnS/ZnS QDs is compared to that of CdS/Mn:ZnS/ZnS QDs. In general, the QD PL is less intense for the doped QDs and can therefore only be observed in a limited intensity range of about two orders of magnitude. This reduced intensity is due to the effective energy transfer from the excitonic QD states to the Mn 3d-shell [20]. This is confirmed by the faster exciton decay of the Mn-doped QDs. For Mn-doped QDs with ATTO633 dye molecules the excitonic lifetime is reduced even further. Now both channels act as energy acceptors, and the energy transfers from the QDs to the Mn ions as well as directly to the dye states. The role of Mn ions as an energy donor has already been revealed in figure 4, where a faster Mn PL decay was observed for the QDs with attached dye molecules in comparison to QDs without.

In figure 6, the transients are depicted for the ATTO633 dye PL in a double logarithmic scale, which allows for a better separation of the different time regimes. The single dye molecules show a mono-exponential decay for several ns (blue triangles). The time behaviour is completely different when the molecules are bound to CdS/ZnS/ZnS QDs (red circles). The characteristic lifetime is now in the  $\mu\text{s}$  range. If dyes are attached to doped CdS/Mn:ZnS/ZnS QDs the decay characteristic changes again substantially (black squares). Up to a few  $\mu\text{s}$  the transients for dye molecules attached to doped and undoped QDs look very similar. The underlying characteristic time is caused by the energy transfer from the QD

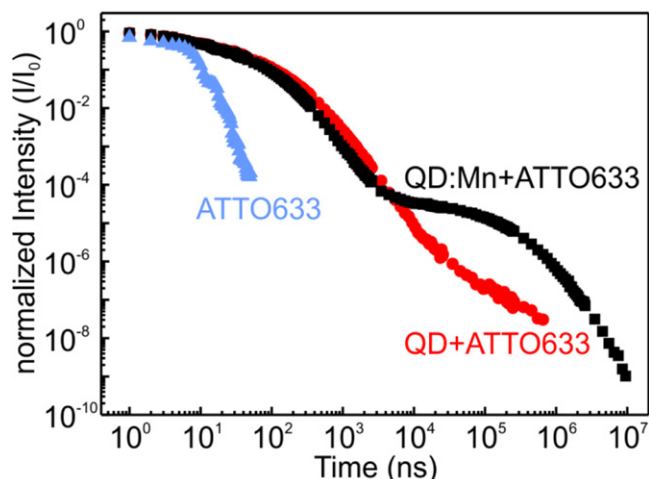


**Figure 6.** Decay curves of the ATTO633 dye PL at 655 nm in the different dye conjugates excited at 355 nm. The decay of free, i.e. unbound, dye molecules (blue triangles), ATTO633-CdS/ZnS/ZnS conjugates (black squares), and ATTO633-CdS/Mn:ZnS/ZnS conjugates (red circles) is shown. The data are plotted in a double logarithmic scale to point out the different time regimes.

excitons to the dye molecules, which is the dominant feeding mechanism in this time window. The small difference in this time window is due to the somewhat faster exciton decay in Mn-doped QDs, which is caused, as mentioned before, by the additional transfer to the Mn states. In the time regime of several  $\mu\text{s}$  up to ms, the distinction between doped and undoped QDs is most striking. Here the dye features a lifetime of several ms, which is identical to the lifetime of the Mn PL.

#### 4. Conclusion

It has been demonstrated that the incorporation of Mn ions as dopants within the ZnS shell of CdS/ZnS core-shell QDs leads to an efficient energy transfer from the excitonic QD states to the Mn states. A multistep growth of the ZnS shell was carried out to control the location of the Mn ions. The effective incorporation of the Mn ions into the QD core-shell structure was confirmed by a clearly observable PL band around 580 nm, which is due to the typical Mn transition. This PL band showed a mono-exponential decay with a lifetime of about 4.6 ms. These Mn-doped CdS/Mn:ZnS/ZnS QDs were further functionalized with organic dye molecules leading to a third fluorescence emitter centre, and therefore to a third PL band. Continuous wave spectra indicated the complex interaction of the different energy states within the QD system. With a thorough investigation of the decay characteristics of the respective PL bands, it was possible to explore the non-radiative energy pathways. We thereby concluded that the QD states act as an energy donor for the Mn as well as for the dye states. Interestingly, the Mn states have a two-fold transfer characteristic, as they also work as an acceptor from the QD states and as a donor for the dye states. In particular, the feeding of the dye states from Mn excitation

led to a tremendous increase in the dye PL lifetime. By choosing a certain dye, and thereby a certain spectral overlap, it was possible to control the lifetime of the dye PL in the range of a few milliseconds.

The attachment of dye molecules to CdS/Mn:ZnS/ZnS QDs led to dye conjugates which could easily be distinguished by means of time-resolved PL measurements from single dye molecules and dye molecules attached to undoped QDs. Mn-doped CdS/Mn:ZnS/ZnS QDs as donors for fluorophores open up a new time regime and potentially allow for the use of dye molecules in complex temporal multiplexing applications. In earlier works [13] we were able to show that the use of undoped QDs leads to the unique and precise determination of the mixing ratio of single and attached dye molecules by time-resolved PL measurements with the same spectral response. Now, we have pointed out that the use of Mn-doped QDs may extend the possibilities of temporal multiplexing even further.

#### Acknowledgments

This work was supported by the Deutsche Forschungsgemeinschaft (DFG GRK 1782 to WJP and WH) and by the European Commission (grant FutureNanoNeeds to WJP). CCC acknowledges a postdoctoral fellowship from the Alexander von Humboldt foundation. NS acknowledges the Higher Education Commission (HEC) Pakistan and GC University Faisalabad (GCUF) Pakistan. We are grateful to M Schneider for his collaboration with the sample measurements.

#### References

- [1] Hötzer B, Medintz I L and Hildebrandt N 2012 Fluorescence in nanobiotechnology: sophisticated fluorophores for novel applications *Small* **8** 2297–326
- [2] Wegner K D and Hildebrandt N 2015 Quantum dots: bright and versatile *in vitro* and *in vivo* fluorescence imaging biosensors *Chem. Soc. Rev.* **44** 4792–834
- [3] Jennings T L *et al* 2011 Reactive semiconductor nanocrystals for chemoselective biolabeling and multiplexed analysis *ACS Nano* **5** 5579–93
- [4] Jezek P, Mahdi F and Garlid K D 1990 Reconstitution of the beef-heart and rat-liver mitochondrial  $\text{K}^+/\text{H}^+$  ( $\text{Na}^+/\text{H}^+$ ) antiporter—quantitation of  $\text{K}^+$  transport with the novel fluorescent-probe, Pbf1 *J. Biol. Chem.* **265** 10522–6
- [5] Graefe A, Stanca S E, Nietzsche S, Kubicova L, Beckert R, Biskup C and Mohr G J 2008 Development and critical evaluation of fluorescent chloride nanosensors *Anal. Chem.* **80** 6526–31
- [6] Abbasi A Z *et al* 2011 How colloidal nanoparticles could facilitate multiplexed measurements of different analytes with analyte-sensitive organic fluorophores *ACS Nano* **5** 21–5
- [7] Berezin M Y and Achilefu S 2010 Fluorescence lifetime measurements and biological imaging *Chem. Rev.* **110** 2641–84
- [8] Masters B R, So P T and Gratton E Multiphoton excitation fluorescence microscopy and spectroscopy of *in vivo* human skin *Biophys. J.* **72** 2405–12



- [9] Geißler D, Linden S, Liermann K, Wegner K D, Charbonnière L J and Hildebrandt N 2014 Lanthanides and quantum dots as Förster resonance energy transfer agents for diagnostics and cellular imaging *Inorg. Chem.* **53** 1824–38
- [10] Hildebrandt N, Wegner K D and Algar W R 2014 Luminescent terbium complexes: superior Förster resonance energy transfer donors for flexible and sensitive multiplexed biosensing *Coord. Chem. Rev.* **273** 125–38
- [11] Gill R, Willner I, Shweky I and Banin U 2005 Fluorescence resonance energy transfer in CdSe/ZnS-DNA conjugates: probing hybridization and DNA cleavage *J. Phys. Chem. B* **109** 23715–9
- [12] Medintz I L, Uyeda H T, Goldman E R and Mattoussi H 2005 Quantum dot bioconjugates for imaging, labelling and sensing *Nat. Mater.* **4** 435–46
- [13] Kaiser U, Aberasturi D J d, Malinowski R, Amin F, Parak W J and Heimbrod W 2014 Multiplexed measurements by time resolved spectroscopy using colloidal CdSe/ZnS quantum dots *Appl. Phys. Lett.* **104** 41901–4
- [14] Busse W, Gumlich H E, Meissner B and Theis D 1976 Time resolved spectroscopy of ZnS: Mn by dye laser technique *J. Lumin.* **12–13**, 693–700
- [15] de Mello Donegá C, Bol A A and Meijerink A 2002 Time-resolved luminescence of ZnS:Mn<sup>2+</sup> nanocrystals *J. Lumin.* **96**, 87–93
- [16] Yu W W and Peng X 2002 Formation of high-quality CdS and other II-VI semiconductor nanocrystals in noncoordinating solvents: tunable reactivity of monomers *Angew. Chem. Int. Ed.* **41** 2368–71
- [17] Chen H Y, Maiti S and Son D H 2012 Doping location-dependent energy transfer dynamics in Mn-doped CdS/ZnS nanocrystals *ACS Nano* **6** 583–91
- [18] Chen O, Shelby D E, Yang Y, Zhuang J, Wang T, Niu C, Omenetto N and Cao Y C 2010 Excitation-intensity-dependent color-tunable dual emissions from manganese-doped CdS/ZnS core/shell nanocrystals *Angew. Chem. Int. Ed.* **49** 10132–5
- [19] Yang Y, Chen O, Angerhofer A and Cao Y C 2008 On doping CdS/ZnS core/shell nanocrystals with Mn *J. Am. Chem. Soc.* **130** 15649–61
- [20] Lin C-A J, Sperling R A, Li J K, Yang T-Y, Li P-Y, Zanella M, Chang W H and Parak W J 2008 Design of an amphiphilic polymer for nanoparticle coating and functionalization *Small* **4** 334–41
- [21] Zhang F, Lees E, Amin F, Rivera\_Gil P, Yang F, Mulvaney P and Parak W J 2011 Polymer-coated nanoparticles: a universal tool for biolabelling experiments *Small* **7** 3113–27
- [22] Fernández-Argüelles M T et al 2007 Synthesis and characterization of polymer-coated quantum dots with integrated acceptor dyes as FRET-based nanoprobe *Nano Lett.* **7** 2613–7
- [23] Kaiser U, Aberasturi D J d, Vazquez-Gonzalez M, Carrillo-Carrion C, Niebling T, Parak W J and Heimbrod W 2015 Determining the exact number of dye molecules attached to colloidal CdSe/ZnS quantum dots in Förster resonant energy transfer assemblies *J. Appl. Phys.* **117** 024701
- [24] Yu W W, Qu L, Guo W and Peng X 2003 Experimental determination of the extinction coefficient of CdTe, CdSe, and CdS nanocrystals *Chem. Mater.* **15** 2854–60
- [25] Yang Y, Chen O, Angerhofer A and Cao Y C 2006 Radial-position-controlled doping in CdS/ZnS core/shell nanocrystals *J. Am. Chem. Soc.* **128** 12428–9
- [26] Labiadh H, Ben Chaabane T, Piatkowski D, Mackowski S, Lalevee J, Ghanbaja J, Aldeek F and Schneider R 2013 Aqueous route to color-tunable Mn-doped ZnS quantum dots *Mater. Chem. Phys.* **140** 674–82
- [27] Norris D J, Efros A L and Erwin S C 2008 Doped nanocrystals *Science* **319** 1776–9
- [28] Norris D J, Yao N, Charnock F T and Kennedy T A 2001 High-quality manganese-doped ZnSe nanocrystals *Nano Lett.* **1** 3–7
- [29] Zu L J, Norris D J, Kennedy T A, Erwin S C and Efros A L 2006 Impact of ripening on manganese-doped ZnSe nanocrystals *Nano Lett.* **6** 334–40
- [30] Erwin S C, Zu L J, Haftel M I, Efros A L, Kennedy T A and Norris D J 2005 Doping semiconductor nanocrystals *Nature* **436** 91–4
- [31] Shim M, Wang C, Norris D J and Guyot-Sionnest P 2001 Doping and charging in colloidal semiconductor nanocrystals *MRS Bull.* **26** 1005–8
- [32] Bawendi M G, Carroll P J, Wilson W L and Brus L E 1992 Luminescence properties of CdSe quantum crystallites—resonance between interior and surface Localized states *J. Chem. Phys.* **96** 946–54
- [33] Goede O and Heimbrod W 2001 Optical properties of (Zn,Mn) and (Cd,Mn) chalcogenide mixed crystals and superlattices *Phys. Status Solidi B* **146** 11–62
- [34] Dexter D L 1953 A Theory of sensitized luminescence in solids *J. Chem. Phys.* **21** 836–50
- [35] Förster T 1949 Experimentelle und theoretische untersuchung des zwischenmolekularen übergangs von elektronenanregungsenergie *J. Phys. Sci.* **4** 321–7
- [36] Kaiser U, Chen L, Geburt S, Ronning C and Heimbrod W 2011 Defect induced changes on the excitation transfer dynamics in ZnS/Mn nanowires *Nanoscale Res. Lett.* **6** 228–32
- [37] Gumlich H E 1981 Electro- and photoluminescence properties of Mn<sup>2+</sup> in ZnS and ZnCdS *J. Lumin.* **23** 73–99
- [38] Goede O, Heimbrod W and Thong D D 1984 Non-exponential ZnS:Mn luminescence decay due to energy transfer *Phys. Status Solidi B* **126** K159–63
- [39] Cao S, Li C, Wang L, Shang M, Wei G, Zheng J and Yang W 2014 Long-lived and well-resolved Mn<sup>2+</sup> ion emissions in CuInS-ZnS quantum dots *Sci. Rep.* **4** 7510
- [40] Resch-Genger U, Grabolle M, Cavaliere-Jaricot S, Nitschke R and Nann T 2008 Quantum dots versus organic dyes as fluorescent labels *Nat. Methods* **5** 763
- [41] van der Meer B W 2013 *FRET—Förster Resonance Energy Transfer* (Weinheim: Wiley) pp 23–62